

Effect of Die Angle on Stress Distribution in Extrusion Process of Aluminum Rod

Rafid Jabbar Mohammed
 Department of Mechanical Engineering
 University of Basrah
 College of Engineering
 Email: rafidjabbar@yahoo.com

Abstract- Type of metal flow and stress distribution in metal extrusion process is a highly complex for the complicated die design. In this work a finite element simulation of Al-1100 rod extrusion was successfully achieved using the commercial finite element code Deform-3D. The results show that the finite element model was successfully simulate the stress distribution in the direct rod extrusion of Al-1100. Besides that the optimum die angle reduces the magnitude of normal, shear, and effective stresses. We can conclude from this study that maximum stresses occur when the rod is with contact with the die at exit stage.

Keywords: extrusion, die angle, stress distribution, aluminum rod.

1. Introduction

Extrusion is the process in which the cross-sectional area of a block of metal is reduced by forcing it to flow through a die with a certain shape under high pressure [1]. There are many factors that affect the extrusion process such as die profile, frictional condition at the tool-workpiece interface, mechanical properties of the material and extrusion ratio [1]. The ratio applies for both direct and indirect extrusion. The extrusion in comparison with other manufacturing methods use in industrial application, has many advantages such as: minimum material waste, high dimensional accuracy, reduction or complete elimination of machining, good surface finish, better mechanical properties of products than those of the original material due to favorable grain flow [2].

The importance of analysis for the extrusion process lies in the determination of forming load, flow characteristics, temperature and state of stress and strain [3].

Typical flow patterns observed in extrusion are shown in Fig.1. Flow pattern S is found in the absence of friction at the container and die interfaces, during extrusion of homogeneous materials. Flow pattern A is obtained in extrusion of homogeneous materials in the presence of friction at the die interface only. In the corner of the leading edge of the billet, a separate metal zone (known as the dead metal zone) is formed between the die face and the container wall. Flow pattern B is obtained in homogeneous materials when there is friction at both die and container interfaces, resulting in an extended dead metal zone. Flow pattern C is observed with billets having inhomogeneous material properties or with non-uniform temperature distribution in the billet; a more extended dead metal zone is formed and the material undergoes a more severe shear deformation at the container wall [4].

Cold extrusion experiments on some solid profiles and simulations using the finite element method (FEM) have been used to investigate the effect of profile complexity on

dead metal zone and metal flow [5]. Studies show that for die cone semi-angles under 45° , the dead metal zone does not form [6-9]. It has been established by various studies that the size and shape of the dead metal zone, and the pattern and homogeneity of flow lines in extrusion are directly related to the die cone angle, to friction at the billet-container interface, and to a lesser extent at the billet-die interface friction [10-13].

In this study a Finite Element Model has been developed to simulate the extrusion process over a variety of die angle. The effects of die angle had a significant role on extrusion analysis.

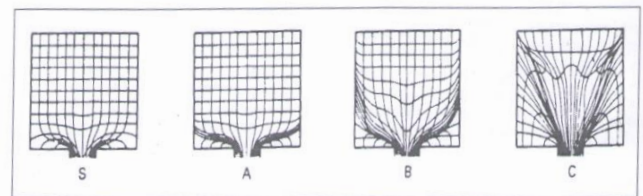


Fig. 1 Different types of metal flow in metal extrusion [4].

2. Analysis of Extrusion Process

Let us use Fig.(2) as a reference in discussing some of the parameters in extrusion. The diagram assumes that both billet and extrudate are round in cross-section. One important parameter is the extrusion ratio, also called the reduction ratio. The ratio is defined [14]:

$$r_x = \frac{A_o}{A_f} \quad (1)$$

where r_x = extrusion ratio; A_o = cross-sectional area of the starting billet, mm² (in²); and A_f = final cross-sectional area of the extruded section, mm² (in²). The value of r_x can be used to determine true strain in extrusion, given that ideal deformation occurs with no friction and no redundant work [14]:

$$\epsilon = \ln r_x = \ln \frac{A_o}{A_f} \quad (2)$$

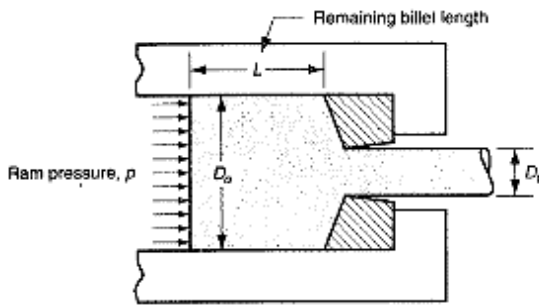


Fig. 2 Pressure and other variables in direct extrusion[14].

Under the assumption of ideal deformation (no friction and no redundant work), the pressure applied by the ram to compress the billet through the die opening can be computed as follows[14]:

$$p = \bar{Y}_f \ln r_x \quad (3)$$

Where \bar{f} = average flow stress during deformation, MPa (lb/in²) and [14]:

$$\bar{Y}_f = \frac{K \epsilon^n}{1+n} \quad (4)$$

Where, k: strength coefficient MPa and n: strain hardening exponent.

In fact, extrusion is not a frictionless process, and the previous equations grossly underestimate the strain and pressure in an extrusion operation.

Friction exists between the die and the work as the billet squeezes down and passes through the die opening. In direct extrusion, friction also exists between the container wall and the billet surface. The effect of friction is to increase the strain experienced by the metal. Thus the actual pressure is greater than that given by equation(3), which assumes frictionless extrusion.

Various methods have been suggested to calculate the actual true strain and associated ram pressure in extrusion. The following empirical equation proposed by Johnson [14] for estimating extrusion strain has gained considerable recognition:

$$\epsilon_x = a + b \ln r_x \quad (5)$$

where x =extrusion strain; and a and b are empirical constants for a given die angle.

The ram pressure to perform indirect extrusion can be estimated based on Johnson's extrusion strain formula as follows[14]:

$$p = \bar{Y}_f \epsilon_x \quad (6)$$

where \bar{f} is calculated based on ideal strain from Equation(2), rather than extrusion strain.

In direct extrusion, the effect of friction between the container walls and billet causes the ram pressure to be greater than for indirect extrusion. Based on this reasoning,

the following formula can be used to compute ram pressure in direct extrusion [14]:

$$p = \bar{Y}_f \left(\epsilon_x + \frac{2L}{D_o} \right) \quad (7)$$

where the ram term $2L/D_o$ accounts for the additional pressure due to friction at the container-billet interface.

Ram force in indirect and direct extrusion is simply pressure p from equation(7) multiplied by billet area A_o [14]:

$$F = p A_o \quad (8)$$

Power required to carry out the extrusion operation is simply[14]:

$$P = Fv \quad (9)$$

Where v is the ram velocity.

3. Material Type and properties

Aluminum-1100 rod with diameter 14mm was chosen to be extruded to final rod diameter of 11.6mm with extrusion ratio of 1.45. The chemical composition of Al-1100 is shown in Table(1), while the important physical and mechanical properties are shown in Table(2) [15].

Table(1) chemical composition of Al-1100

Element	%	element	%
Al	99.6	Mn	0.03
Cu	0.05	Si	0.25
Fe	0.35	Ti	0.03
Mg	0.03	Zi	0.05
V	0.05		

Table(2) physical and mechanical properties of Al-110

Property	Value
Density	2.71 gm/cm ³
Brinell Hardness	23
Ultimate Tensile Strength	89.6 Mpa
Tensile Yield Strength	34.5 Mpa
Elongation at Break	35.00% @ Thickness 1.59 mm 45.00% @ Diameter 12.7 mm
Modulus of Elasticity	68.9 Gpa
Poisson's Ratio	0.33
Shear Modulus	26 Gpa
Shear Strength	62.1 Mpa

4. Finite Element Modeling of rod Extrusion

In this work the finite element code Deform-3D V6.1 was used in modeling and analysing the direct extrusion process of AL1100 bar. According to symmetry quarter model was considered, tetraheadreal element type with 13312 number of element and 3086 nodes were chosen in simulating the aluminum rod. Since the present study concentrate on the stress distribution on the extruded bar, a rigid die and punch

were considered to ignore any deformation in the die and punch. Figure(3) shows the die-punch setup and the 3D finite element model.

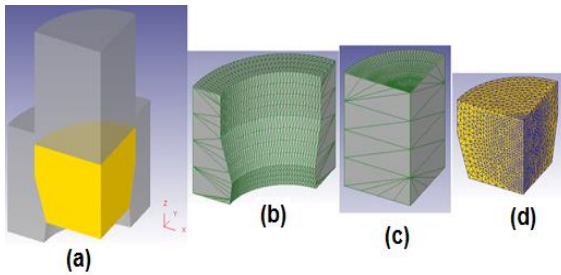


Fig. 3 Die-Punch setup: a. 3D punch –die setup b. die c. punch d.3D FE model

5. Results and Discussion

Type of metal flow and stress distribution in metal extrusion process is a highly complex for the complicated die design. Therefore finding the optimum die angle is most important task in extrusion process. Figures(4) to (6) show the maximum stress distribution along the x, y, and z-axis respectively at different die angles. From these figures it seems that 45° die angle is the optimum angle and according to equations (7), (8), and (9) minimum power consumption was needed compared with the other die angles. Similarly for the maximum shear stress in xy, yz, and zx planes, Figures (7), (8), and (9) respectively, die angle of 45° produce minimum values for the maximum shear stress compared with other die angles. The same notice was observed with the distribution of maximum effective stress and maximum principal stress as shown from Figures (10) and (11). Figures (12) and (13) show the contour plot of effective stress distribution for die angle 45° at different extrusion times which show that maximum effective stress occurs at die exit.

6. Conclusions

From the present paper we can conclude the following notices:

The finite element model was successfully simulated the stress distribution in the direct rod extrusion of Al-1100. Also this study demonstrated that optimum die angle reduce the magnitude of normal, shear, and effective stresses. This paper showed that maximum stresses occur when the rod is with contact with the die at exit stage.

7. References

[1] M. Bakhshi-Jooybari, M. Saboori, M. Noorani-Azad, S.J. Hosseini-pour, " Combined upper bound and slab method, finite element and experimental study of optimal die profile in extrusion", *Materials and Design* 28 (2007) 1812–1818.
 [2] A. Farhoumand, R. Ebrahimi, "Analysis of forward-backward-radial extrusion process", *Materials and Design* 30 (2009) 2152–2157.
 [3] Yang DY, Kim KJ. " Design of processes and products through simulation of three-dimensional extrusion", *J Mater Process Technol* 2007;191:2–6.

[4] M. Bauser, G.Sauer, K. Siegert (ed), *Extrusion*, 2nd edition, ASM International, 2001.
 [5] S.Z. Qamar, " FEM study of extrusion complexity and dead metal zone", *Archives of Materials Science and Engineering*, Volume 36, Issue 2, April 2009, Pages (110-117).
 [6] T. Kloppenborg, M. Schikorra, J.P. Rottberg, A.E. Tekkaya, " Optimization of die topology in extrusion processes", *Advanced Materials Research* 43 (2008) 81-88.
 [7] G. Liu, J. Zhou, J. Duszczak, " FE Analysis of metal flow and weld seam formation in a porthole die", *Journal of Materials Processing Technology* 200/1-3 (2008) 185-198.
 [8] M. Schikorra, M. Kleiner, " Simulation-based analysis of composite extrusion processes", *CIRP Annals – Manufacturing Technology* 56/1 (2007) 317-320.
 [9] M.P. Reddy, " Analysis and design optimization of aluminum extrusion dies", *Proceedings of the 8th Aluminum Extrusion Technology Seminar*, Orlando, USA, 2 (2004) 171-178.
 [10] A.R. Eivani, T.A. Karimi, " The effect of dead metal zone formation on strain and extrusion force during equal channel angular extrusion", *Computational Materials Science* 42 (2008) 14-20.
 [11] H. Sano, T. Ishikawa, N. Yukawa, Y. Yoshida, T. Kaneko, " Effect of extrusion mode and die shape on billet skin behaviour in aluminum extrusion", *Journal of Japan Institute of Light Metals* 58/5 (2008) 183-188.
 [12] H.H. Jo, S.K. Lee, C.S. Jung, B.M. Kim, " A non-steady state Fe analysis of AL tubes hot extrusion by a porthole die", *Journal of Materials Processing Technology* 173/2 (2006) 223-231.
 [13] L. Donati, L. Tomesani, " The effect of die design on the production and seam weld quality of extruded aluminum profiles", *Journal of Materials Processing Technologies* 164-165 (2005) 1025-1031.
 [14] Mikell P. Groover "Fundamentals of Modern Manufacturing: Materials, processes, and Systems" 3rd edition, John Wiley & Sons, Inc, 2007.
 [15] ASTM B491, "Standard specification for Aluminum and Aluminum-Alloy extruded round tubes for general purpose application", 2006.

Symbol List:

- rx: extrusion ratio
 Ao: cross-section area of starting billet, mm² (in²)
 Af: final cross-section area of extruded section, mm² (in²)
 ε : true strain
 Do: diameter of starting billet, mm (in)
 Df: diameter of extruded section, mm (in)
 L: remaining billet length, mm (in)
 p : ram pressure, MPa (lb/in²)
 f: average flow stress during deformation, MPa (lb/in²)
 k: strength coefficient, MPa (lb/in²)
 n: strain hardening exponent
 x=Johnson's extrusion strain
 a and b: empirical constants for a given die angle in Johnson's relation
 F: ram force, N (lb)
 P: Power required to carry out the extrusion operation, Watt (HP)
 v: ram velocity, mm/s (in/s)

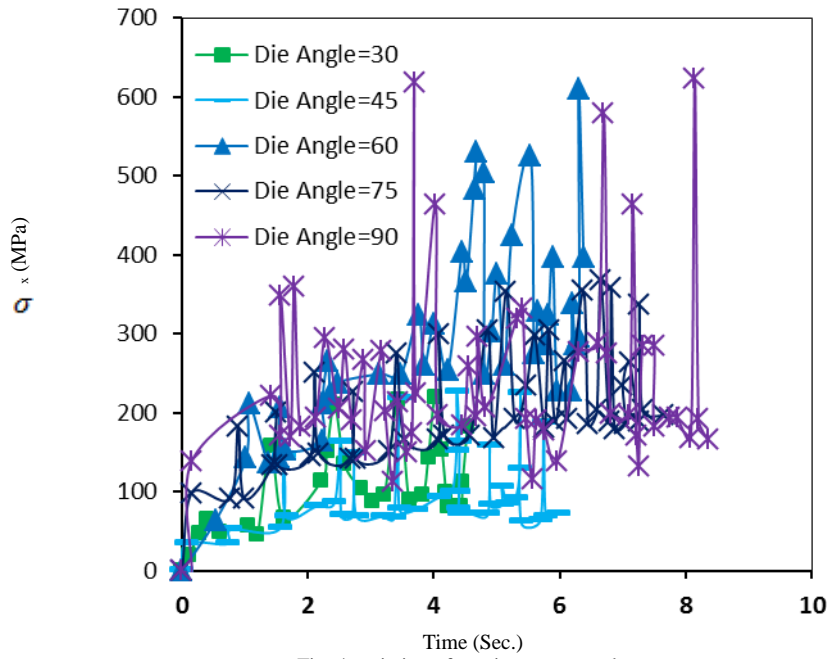


Fig. 4 variation of maximum stress along x-axis with time for different die angles.

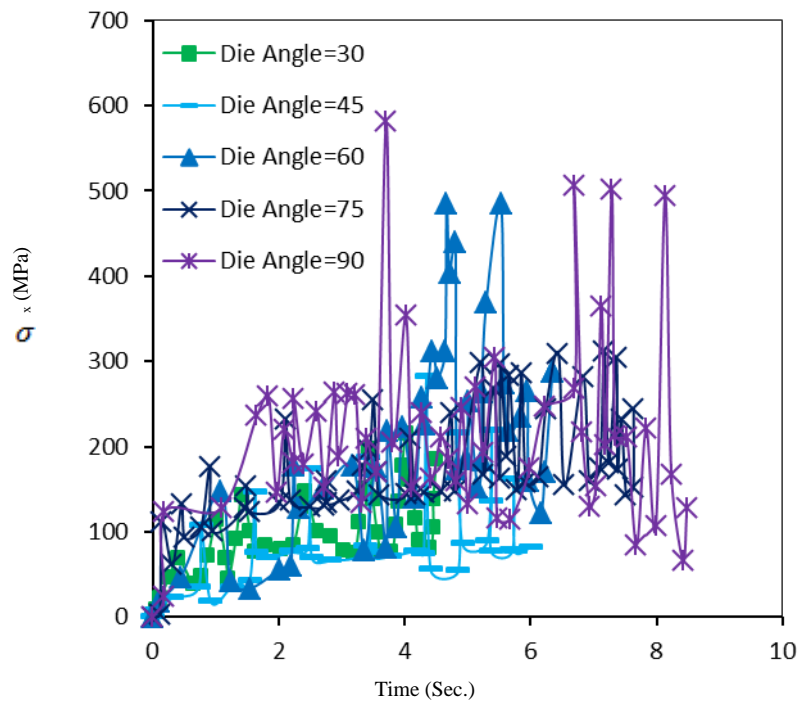


Fig. 5 variation of maximum stress along y-axis with time for different die angles.

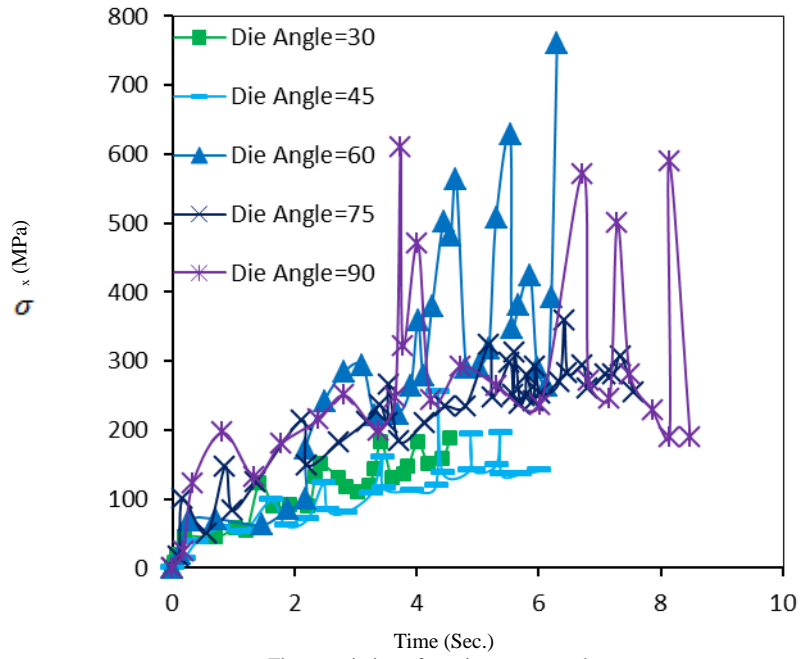


Fig. 6 variation of maximum stress along z-axis with time for different die angles.

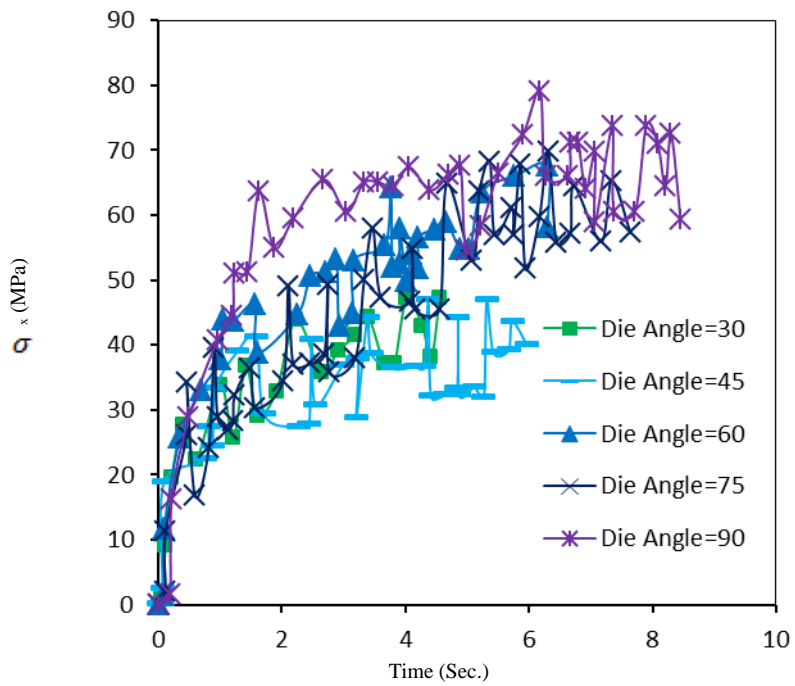


Fig. 7 variation of maximum xy shear stress with time for different die angles.

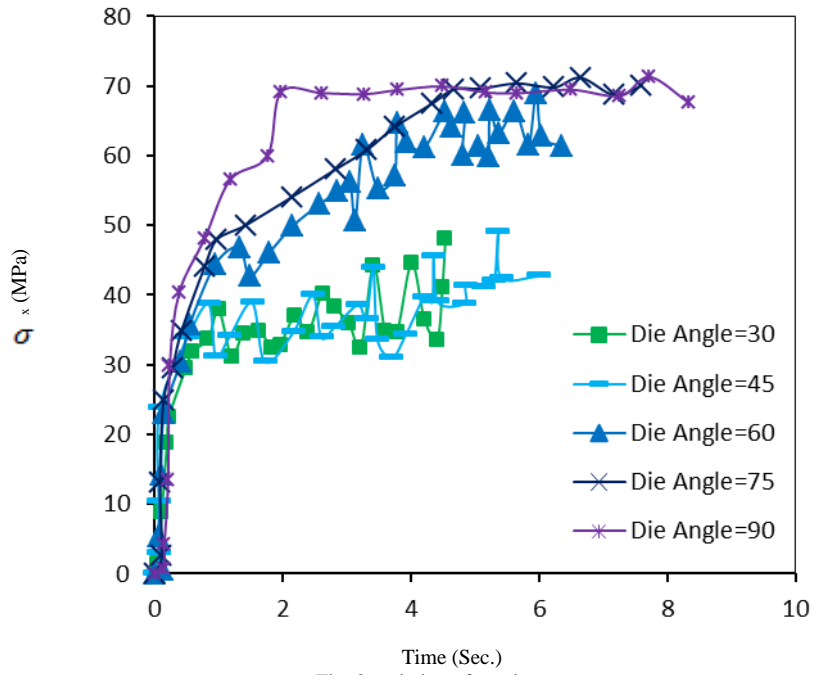


Fig. 8 variation of maximum yz shear stress with time for different die angles.

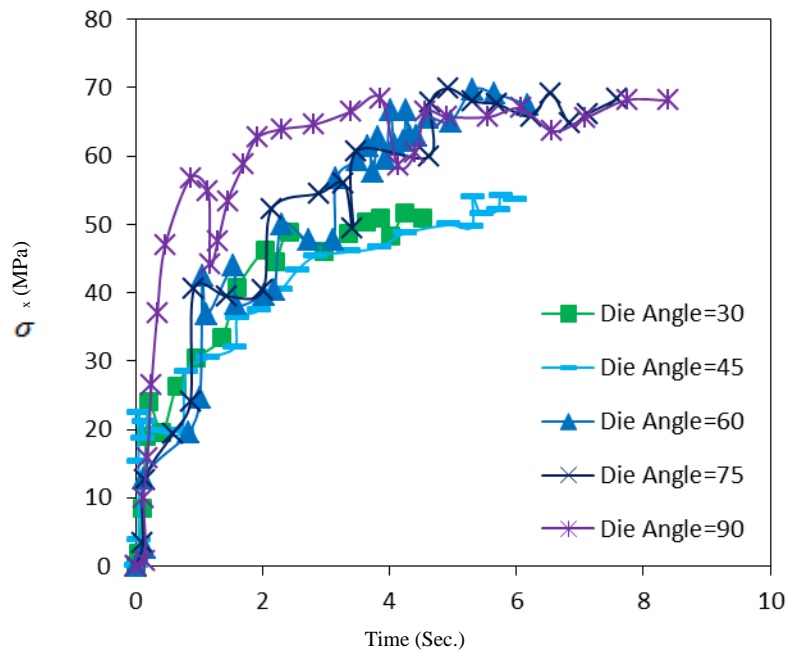


Fig. 9 variation of maximum zx shear stress with time for different die angles.

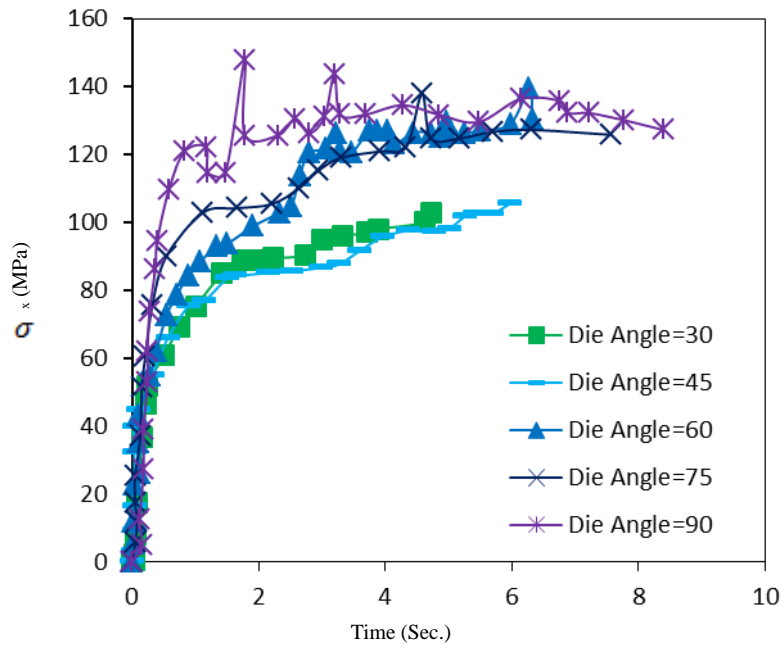


Fig. 10 variation of effective stress with time for different die angles.

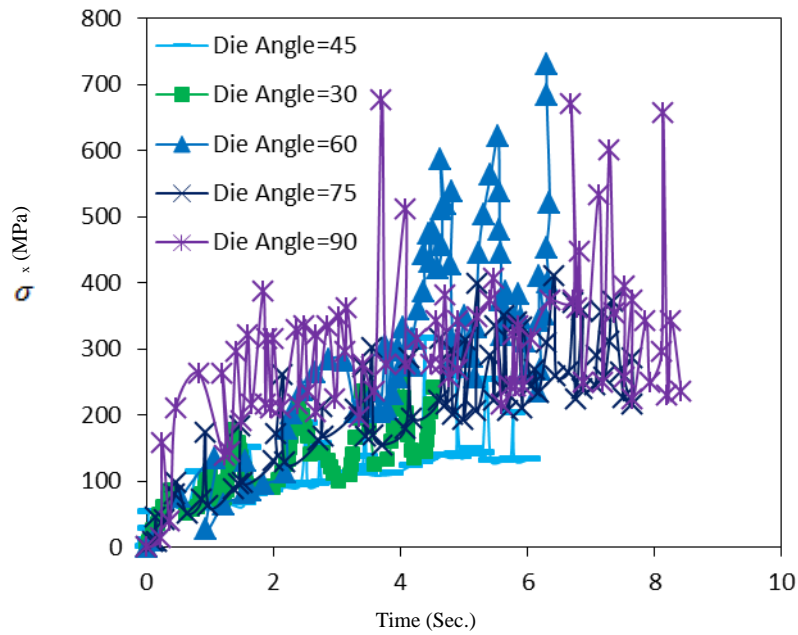


Fig. 11 variation of maximum principal stress with time for different die angles.

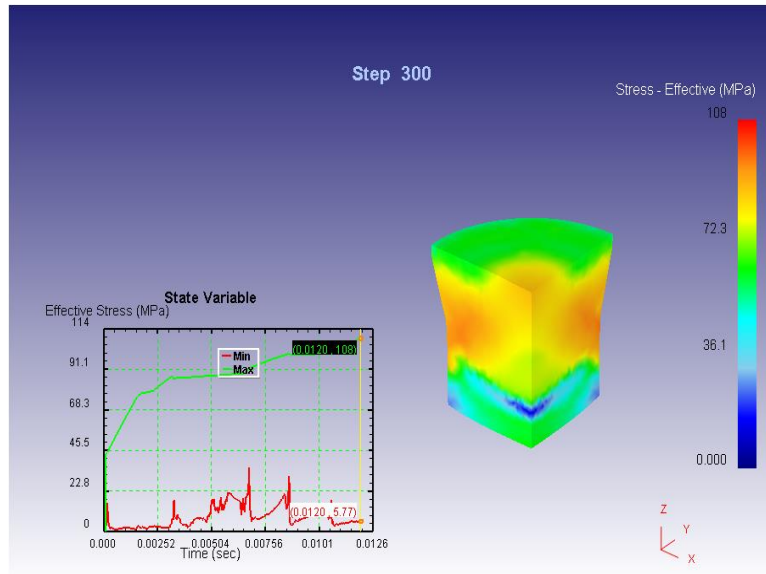


Fig. 12 Contour plot of effective stress distribution after 0.012 sec. of extrusion time.

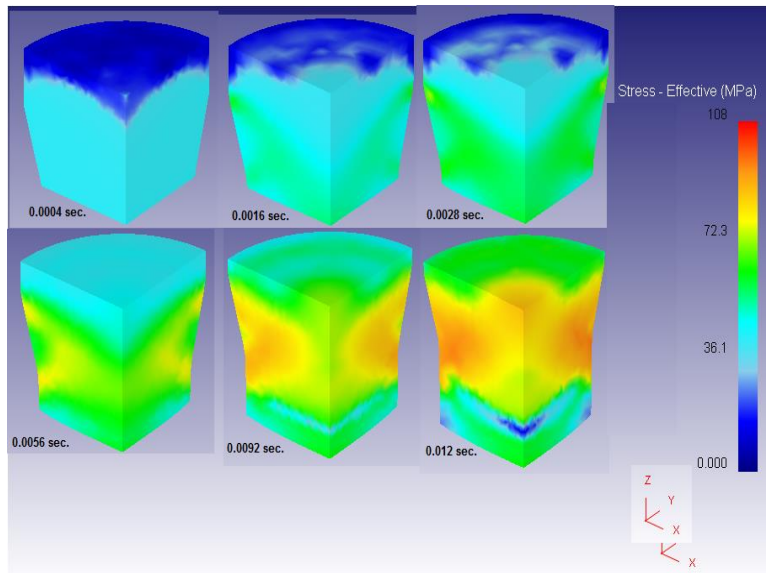


Fig. 13 Contour plot of effective stress distribution at different extrusion times.